文章编号：1001-9014(2020)04-0430-04

DOI:10.11972/j.issn.1001-9014.2020.04.006

Photo-excited tunable metamaterial and its sensing application

LIU Jing[1*], SHEN Jing-Ling[2], ZHANG Cun-Lin[1,2*], ZHAO Yue-Jin[1]

(1. School of Optoelectronics, Beijing Institute of Technology, Beijing 100081, China;
2. Key Laboratory of Terahertz Optoelectronics, Ministry of Education, Capital Normal University, Beijing 100048, China)

Abstract: A terahertz photo-excited tunable metamaterial sensor is investigated. It is composed of a hybrid metal-semiconductor structure (which is a split ring resonator (SRR)) and a flexible polyimide substrate. Silicon is filled in the gaps of the structure. Simulation results reveal that the conductivity of the semiconductor component can be tuned by changing the external pump light's power, resulting in resonant peak shift of the composited metamaterial structure. The electric field and surface current density distributions of this structure under different resonant frequencies are also analyzed. The physical mechanism of this device has been further discussed. Moreover, the resonant peak will be red-shift as the concentration of the surrounding environment (calcium chloride, $CaCl_2$) increases, and the sensitivity is 11.4 GHz/M, which makes it a possible application in liquid sensing in terahertz region.

Key words: terahertz, metamaterial, liquid sensor

PACS: 41.20.Jb, 78.20.-e, 78.67.-n

光调制超材料及其传感应用

刘 婧[1*], 沈京玲[2], 张存林[1,2*], 赵跃进[1]

(1. 北京理工大学 光电学院,北京 100081;
2. 首都师范大学 太赫兹光电子学教育部重点实验室,北京 100048)

摘要:研究了一种太赫兹光调制超材料传感器。该器件由金属-半导体复合结构(开口谐振环(SRR))和柔性聚酰亚胺衬底组成。光敏硅材料填充在器件上方的两个开口处。模拟结果表明,通过改变外激励泵浦光的功率,光敏硅的电导率发生改变,从而实现对复合超材料结构谐振峰的调制。进一步分析该结构在谐振频率下的电场和表面电流密度分布情况,讨论了其物理机制。此外,随着待测溶液(氯化钙)浓度变化,传感器谐振峰发生红移,其灵敏度为 11.4 GHz/M。该器件可作为太赫兹波段液体传感器使用。

关 键 词:太赫兹;超材料;液体传感器

中图分类号:TB34;O441 **文献标识码**:A

Introduction

In recent years, metamaterials have attracted great attention due to their unique properties[1-5]. Thus, some actively tunable composite metamaterial devices based on a split-ring resonator (SRR) have been investigated in terahertz region [6-12]. These structures with better device performances are highly desired for sensing applications, especially in bio-medical region[13].

Ionic solution, such as calcium chloride ($CaCl_2$), plays an essential role in many biochemical processes[14-16]. So it is necessary to study its optical properties for practical application. However, few works has been done about it in terahertz region. Here, we firstly measured the dielectric responses of $CaCl_2$ solutions with different concentrations (up to 3 mol/L) for further sensing simulation.

In this work, a novel terahertz photo-excited tunable metamaterial switch is investigated. Its resonant frequencies can be modulated by variation of external light intensity. Furthermore, the gap of this structure can be equivalent to a capacitor, and LC resonance occurs as a re-

Received date: 2019-09-29, **revised date**: 2020-02-24 **收稿日期**:2019-09-29,**修回日期**:2020-02-24

Foundation items: Supported by the Beijing Advanced Innovation Center for Imaging Theory and Technology (19530012003)

Biography: LIU Jing (1987-), female, Ph. D. candidate. Research area focus on terahertz waveguide spectroscopy etc.

* **Corresponding author**: newone_kaka@163.com, cunlin_zhang@cnu.edu.cn

sult, which is sensitive to its surrounding dielectric environment. Therefore, this structure can also achieve a sensing application by changing the concentration of the injected ionic solution.

1 Structure design and analysis

The schematic diagram of the proposed structure's unit cell is shown in Fig. 1 (a). It consists of a split ring copper resonator on the top layer on a polyimide layer. The permittivity of the polyimide is set to be 3.5. The geometric parameters of the structure are shown as follows: p_x=p_y=120 μm, l_x=60 μm, l_y=90 μm, g_1=4 μm, g_2=18 μm, w_1=6 μm, w_2=12 μm, w_3=3 μm, h=6 μm. The thickness of the copper lays t_1 is 0.4 μm, while the thickness of the polyimide layer t_2 is 2 μm. We filled the two gaps on the top of the material with silicon. The configuration of testing is shown in Fig. 1 (b). When irradiated by an external pump laser on the SRR array, light-generated carriers existed in the silicon region. The structure is illuminated by terahertz wave whose electric field is along the y direction. As the power of external light increases, the carrier concentration on Si increases, and it will lead to the increase of its conductivity [8-9]. The silicon conductivity can reach the magnitude of 10^5 S/m, which is close to metallic conductivity when the light power is high enough. The CST studio simulation results with various silicon conductivities are presented in Fig. 2. For the structure illuminated by terahertz wave whose electric field was perpendicular to the top two split gaps, the resonant dip located in 1.139 THz when the conductivity of the silicon was 1 S/m. With the increase of the silicon conductivity, the frequency of the resonant dip gradually shifted to 0.8 THz as the silicon conductivity reached 300000 S/m which was equivalent to the laser light with an intensity of 6111 μm/cm^2 [17]. The frequency of the resonant dip varied from 1.14 to 0.8 THz as the silicon conductivity increased from 1 to 300000 S/m, which is shown in Fig. 2(a). For the structure illuminated by terahertz wave whose electric field was parallel to the top two split gaps, as shown in Fig. 2(b), the two resonant dips located in 0.645 THz and 1.716 THz when the conductivity of the silicon was 1 S/m, and slightly shifted to one resonant dip in 1.256 THz as silicon conductivity varied to 300000 S/m. Figure 3 (a-e) show the electric field and surface current density distributions of the proposed structure when terahertz wave was perpendicular or parallel to the top two split gaps at the resonant frequencies. As the silicon conductivity increased and reached the magnitude of 10^5 S/m, which was close to metallic conductivity, the silicon component became a conducting region allowing the surface current at the silicon-copper interface to bridge the split gap, and thus the two top gaps of the SRRs were short-circuited [8].

2 Sensing application

The dielectric responses of $CaCl_2$ solutions with different concentrations (up to 3 mol/L) were measured by a typical terahertz time domain spectroscopy system in the range of 0.2~1.5 THz, which are shown in Fig. 4.

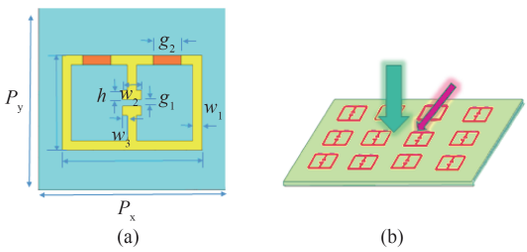

Fig. 1　Schematic diagram of (a) the proposed photosensitive structure, and (b) laser pump testing configuration
图1　(a)光敏超材料结构,(b)光泵浦测量示意图

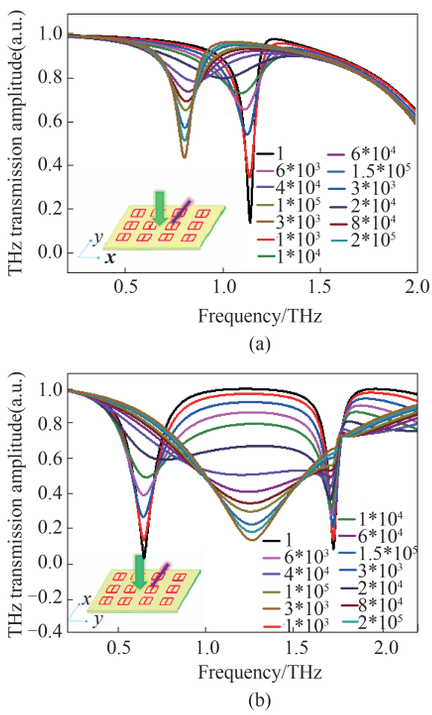

Fig.2　Transmission spectrum of metamaterial structure for various silicon conductivities when electric field of terahertz wave was (a) perpendicular, and (b) parallel to the top two split gaps
图2　不同电导率下超材料结构的透射谱(a)太赫兹电场方向垂直于顶端开口方向,(b)平行于顶端开口方向

The real parts (ε') and imaginary parts (ε'') of the complex permittivity can be calculated for further sensing simulation [18]. Figure 5 shows the simulation results of $CaCl_2$ with different concentration without light irradiation. The result in pure de-ionic water is simulated as a reference. As the concentration increased from 0 to 3 mol/L, the resonant dip presented red-shifted from 1.009 to 0.975 THz, which indicated that this structure can be an efficient sensor for further application. The simulation results of frequency shifts for different $CaCl_2$ concentrations are illustrated in Fig. 6. The growth of frequency shift shows positive correlation with the increasing of molar concentration. The sensitivity in terms of molar concentration of $CaCl_2$ yields 11.4 GHz per M, which indicated that this structure can be an effected sensor monitoring concentrations of ionic solution. The sensitivity can be further optimized by method such as changing the geometry of the pattern and substrate config-

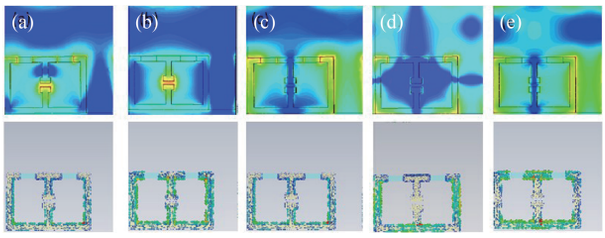

Fig. 3 Electric field and surface current density distributions of the proposed structure when terahertz wave was perpendicular to the top two split gaps (a) located at 1. 139 THz when the conductivity of Si σ = 1 S/m, (b) located at 0. 8 THz when σ = 300 000 S/m. Electric field and current distributions when terahertz wave was parallel to the top two split gaps, (c) located at 0. 645 THz, (d) 1. 716 THz when σ = 1 S/m, and (e) located at 1. 256 THz when σ = 300 000 S/m

图3 当入射的太赫兹波垂直于结构顶端两开口方向(a)f=1. 139 THz, σ=1 S/m,(b)f=0. 8 THz, σ=300 000 S/m,当入射太赫兹波平行于结构顶端两开口方向,(c)f=0. 645 THz, σ=1 S/m,(d)f=1. 716 THz, σ=1 S/m,(e)f=1. 256 THz, σ=300 000 S/m电场与表面电流密度分布

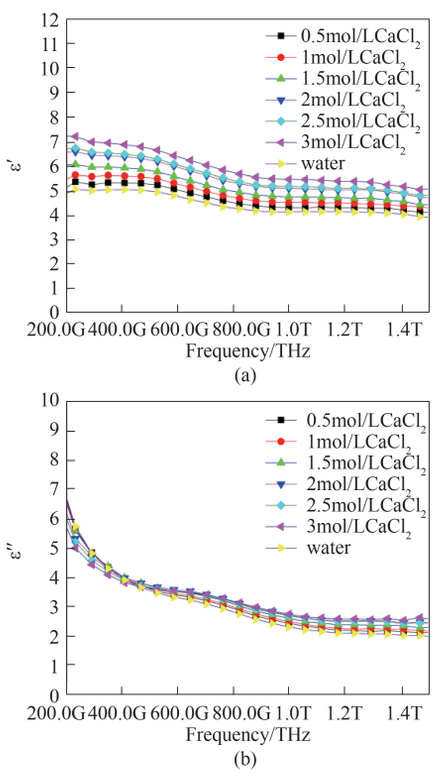

Fig. 4 (a) Real parts (ε'), and (b) imaginary parts (ε'') of the complex permittivity of $CaCl_2$ solutions with different concentrations

图4 $CaCl_2$溶液复介电函数的(a)实部(ε'),(b)虚部(ε'')

uration.

3 Conclusion

In this work, a terahertz photo-excited tunable metamaterial sensor is investigated, and the resonant frequency of this switch can be modulated by variation of external light intensity and changing the permittivity of the surrounding material. This sensor is composed of a hybrid metal-semiconductor structure and a flexible polyimide substrate. Silicon is filled in the gaps of the structure. Simulation results reveal that the conductivity of the semiconductor component can be tuned by changing the external pump light's power, resulting in resonant peak shift of the composite metamaterial structure. The electric field and current density distributions of this structure under different resonant frequencies are also analyzed. The physical mechanism of this device has been further discussed. Moreover, the resonant peak will be red-shift as the permittivity of $CaCl_2$ increases, and the sensitivity is 11. 4 GHz per M. This work will contribute to qualitative and quantitative study in trace sensing in terahertz region, especially for non-destructive testing of low-density or thin-film biological samples.

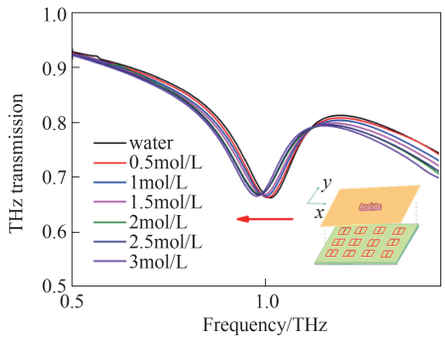

Fig. 5 Peak responses of the sensor for different permittivities and the inset figure is the schematic diagram of the proposed structure coated with analyte

图5 不同介电函数下传感器的峰值响应,其中内置图片为传感结构示意图

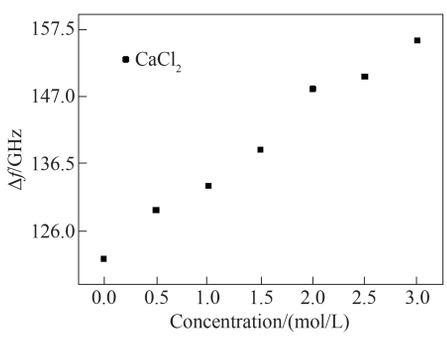

Fig. 6 Frequency shifts for different $CaCl_2$ molar concentrations

图6 不同摩尔浓度$CaCl_2$对应的频移

References

[1] Chen H T, Padilla W J, Zide J M, *et al*. Active terahertz metamaterial devices [J]. *Nature*, 2006, **444**(7119): 597-600.
[2] Singh R, Wei C, Alnaib I, *et al*. Ultrasensitive THz sensing with high-Q Fano resonances in metasurfaces [J]. *Applied Physics Letters*, 2014, **105**(17): 41-48.
[3] Pendry J B, Schurig D, Smith D R. Controlling electromagnetic fields [J]. *Science*, 2006, **312**(5781): 1780-1782.
[4] Ulf L. Optical conformal mapping [J]. *Science*, 2006, **312**(5781): 1777-1780.
[5] Zhang S, Park Y-S, Li J, *et al*. Negative Refractive Index in Chiral Metamaterials [J]. *Physical Review Letters*, 2009, **102**(2): 023901.
[6] Shen X, Cui T J. Photoexcited broadband redshift switch and strength modulation of terahertz metamaterial absorber [J]. *Journal of Optics*, 2012, **14**(11): 114012.

[7] Nian-Hai S, Maria M, Mutlu G, *et al*. Optically implemented broadband blueshift switch in the terahertz regime [J]. *Physical Review Letters*, 2011, **106**(3): 037403.
[8] Wang G, Zhang J, Bo Z, *et al*. Photo-excited terahertz switch based on composite metamaterial structure [J]. *Optics Communications*, 2016, **374**: 64-68.
[9] Zhang J, Wang G, Bo Z, *et al*. Photo-excited broadband tunable terahertz metamaterial absorber [J]. *Optical Materials*, 2016, **54**: 32-36.
[10] George J, Menon C S. Electrical and optical properties of electron beam evaporated ITO thin films [J]. *Surface & Coatings Technology*, 2000, **132**(1): 45-48.
[11] Rahm M, Li J S, Padilla W J. THz wave modulators: A brief review on different modulation techniques [J]. *Journal of Infrared Millimeter & Terahertz Waves*, 2013, **34**(1): 1-27.
[12] Zhu J, Han J, Zhen T, *et al*. Thermal broadband tunable Terahertz metamaterials [J]. *Optics Communications*, 2011, **284**(12): 3129-3133.
[13] Ling X, Xiao Z, Zheng X. Tunable terahertz metamaterial absorber and the sensing application [J]. *Journal of Materials Science Materials in Electronics*, 2017, **29**(1): 1-7.
[14] Hewish N A, Neilson G W, Enderby J E. Environment of Ca^{2+} ions in aqueous solvent [J]. *Nature*, 1982, **297**(5862): 138-139.
[15] Dai Q, Xu J J, Li H J, *et al*. Ion association characteristics in $MgCl_2$ and $CaCl_2$ aqueous solutions: a density functional theory and molecular dynamics investigation [J]. *Molecular Physics*, 2015, **113**(22): 3545-3558.
[16] Kann Z R, Skinner J L. Low-frequency dynamics of aqueous alkali chloride solutions as probed by terahertz spectroscopy [J]. *Journal of Chemical Physics*, 2016, **144**(23): 1.
[17] Gu J Q. Research on terahertz metamaterials[D]. Tianjin University, 2010.
[18] Vinh N Q, Sherwin M S, Allen S J, *et al*. High-precision gigahertz-to-terahertz spectroscopy of aqueous salt solutions as a probe of the femtosecond-to-picosecond dynamics of liquid water[J]. *The Journal of Chemical Physics*, 2015, **142**(16): 164502.